

## Spotting imprints of dark matter in the extragalactic gamma-ray sky with photon counts statistics

---

Hannes-S. Zechlin\*<sup>a</sup>, Silvia Manconi<sup>ab</sup> and Fiorenza Donato<sup>ab</sup>

<sup>a</sup>*Istituto Nazionale di Fisica Nucleare, Sezione di Torino, via P. Giuria, 1, I-10125 Torino, Italy*

<sup>b</sup>*Dipartimento di Fisica, Università di Torino, via P. Giuria, 1, I-10125 Torino, Italy*

*E-mail:* [zechlin@to.infn.it](mailto:zechlin@to.infn.it)

Apart from resolved gamma-ray emitters, the extragalactic gamma-ray background (EGB) comprises emission from potentially undetected sources and may therefore serve as a valuable tool for their detection. While the classical approach of EGB decomposition manifests in combined spectral fits of individual contributions, statistical methods have been proven to be even more sensitive. In this contribution, we summarize recent attempts of using 1-point photon counts statistics for decomposing the EGB detected with Fermi-LAT, focusing on point-source contributions and the diffuse isotropic background contribution. For the first time, we generalize the analysis to incorporate a potential contribution from annihilating dark matter. This allows the derivation of new competitive upper limits on the dark matter self-annihilation cross section, which are complementary to upper limits obtained with other indirect detection methods.

*35th International Cosmic Ray Conference — ICRC2017  
10–20 July, 2017  
Bexco, Busan, Korea*

---

\*Speaker.

## 1. Introduction

With the Large Area Telescope (LAT) on board the Fermi Gamma-ray Space Telescope (Fermi), significant progress in understanding the non-thermal gamma-ray sky has been made. The total gamma-ray emission composes into bright contributions from our Galaxy, while all other gamma rays from outside the Galaxy accumulate into another major component, known as the extragalactic gamma-ray background (EGB) [1]. The EGB disseminates into point sources (PSs) and an effectively isotropic diffuse background contribution, the IGRB. The EGB has been detected with the LAT at Galactic latitudes  $|b| > 20^\circ$  for energies between 100 MeV and 820 GeV with unprecedented precision [2].

Most of the PSs individually resolved in source catalogs such as the Fermi Large Area Telescope Third Source Catalog (3FGL) [3] have been associated with blazars. In general, different source populations distinguish themselves by their intrinsic source count distributions  $dN/dS$ , denoting the number of sources  $N$  per solid angle element  $\Delta\Omega$  with integral fluxes in the interval  $(S, S+dS)$ . Phenomenologically, source count distributions can be obtained from data-driven models (describing blazars, for instance), derived from basic principles of source-intrinsic gamma-ray production and cosmological evolution. Extrapolating those models to fainter flux regimes suggests numerous sources beyond the detection sensitivity of current gamma-ray catalogs [4, 5]. The IGRB is thus expected to be at least partly composed of unresolved faint PS populations. As opposed to PS contributions, the IGRB might contain purely diffuse components, among them diffuse gamma-rays originating from cosmic-ray interactions with the intergalactic medium or the annihilation or decay of dark matter (DM) particles in DM halos around galaxies [6]. Existence and properties of DM are, however, still elusive and would pose a tantalizing discovery.

In contrast to dissecting the EGB by means of individual source detections and intensity measurements, statistical methods have been demonstrated to be capable of measuring  $dN/dS$  and diffuse EGB components [7, 8, 9, 10]. In Refs. [11, 12], henceforth Z16a and Z16b, respectively, we have shown that the 1-point probability distribution function (1pPDF) of counts maps, i.e. the PDF of photon counts as distributed in a pixelized map, serves as a unique tool for providing precise measurements of  $dN/dS$  and the EGB's composition. Statistical measurements are not only complementary to standard catalog procedures, but they also significantly increase the sensitivity for detecting PS populations.

In this contribution, we extend the analysis setup as applied in Z16a,b to incorporate an additional component representing a Galactic DM halo. On the basis of different Galactic foreground emission models, we investigate the sensitivity reach of the 1pPDF method with regard to constraining the DM self-annihilation cross section  $\langle\sigma v\rangle$ .

## 2. The 1pPDF Method and DM

The method of deriving the 1pPDF, its implementation, and its application to Fermi-LAT data are discussed in Z16a,b. Here, we extend the model of the gamma-ray sky to an additional component, i.e. we consider a superposition of four individual components: (i) an isotropic distribution of gamma-ray point sources, described by their differential source-count distribution  $dN/dS$ , (ii) a diffuse component of interstellar emission, corresponding to the Galactic foreground emission, (iii)

a distribution of DM, representing a typical Galactic DM halo, and (iv) a diffuse component accounting for all contributions indistinguishable from purely diffuse isotropic emission. The  $dN/dS$  distribution was incorporated with a multiply broken power law (MBPL), with its fit parameters comprising the overall normalization,  $N_b$  break positions, and therefore  $N_b + 1$  power-law components between the breaks. The interstellar emission model (IEM) was incorporated with spatial and spectral templates. The overall normalization,  $A_{\text{gal}}$ , of the IEM template was kept a free fit parameter. Likewise, the component of Galactic DM was included as a template with a free overall normalization parameter  $A_{\text{dm}}$ . The diffuse isotropic background emission was assumed to follow a power law spectrum (photon index  $\Gamma = 2.3$ ), with its integral flux,  $F_{\text{iso}}$ , serving as the free normalization parameter.

The total photon contribution to map pixel  $p$  from the diffuse components (ii)-(iv) is represented by the sum of each individual component. Generically, the 1pPDF can be derived from probability generating functions, see Z16a, Section 2, for details. The total diffuse component is given by the generating function  $\mathcal{G}^{(p)}(t) = \exp[x_{\text{diff}}^{(p)}(t - 1)]$ , where  $t \in \mathbb{R}$  is an auxiliary variable and  $x_{\text{diff}}^{(p)}$  denotes the number of photon counts expected in pixel  $p$  from all diffuse contributions. The quantity  $x_{\text{diff}}^{(p)}$  is thus given by

$$x_{\text{diff}}^{(p)} = A_{\text{gal}}x_{\text{gal}}^{(p)} + A_{\text{dm}}x_{\text{dm}}^{(p)} + \frac{x_{\text{iso}}^{(p)}}{F_{\text{iso}}}F_{\text{iso}}, \quad (2.1)$$

generalizing Eq. 11 in Z16a, where  $x_b^{(p)}$ ,  $b \in [\text{gal}, \text{dm}, \text{iso}]$ , are the numbers of expected photon counts from the individual contributions (ii)-(iv).

The general 1pPDF routine is based on Markov Chain Monte Carlo (MCMC) sampling of a likelihood function that is given by a product over the probabilities of finding the number  $k_p$  of measured counts in pixel  $p$ . Parameters are estimated from the profile likelihood (frequentist approach).

## 2.1 IEM templates

In this work, we consider 4 different IEMs in order to model the Galactic foreground emission. Our benchmark template adopts the official spatial and spectral template as provided by the Fermi LAT Collaboration for the `Pass 8` analysis framework (see Section 3). In addition, we compare analyses using the models A, B, and C as used in Ref. [2] to bracket the systematic uncertainties of the IGRB analysis.

## 2.2 The DM component

Accumulating evidence, mainly provided by complementary astrophysical observations, suggests the dominant matter component in the Universe to be a form of non-baryonic, collisionless, and cold dark matter (DM) [13]. In the standard scenario structures form hierarchically, leading to massive and largely extended DM halos hosting galaxies like our Milky Way. DM composed of new elementary particles such as weakly interacting massive particles (WIMPs) can self-annihilate or decay, yielding line-like features and a continuous spectrum of gamma-rays unavoidably produced by secondary interactions from annihilation final states.

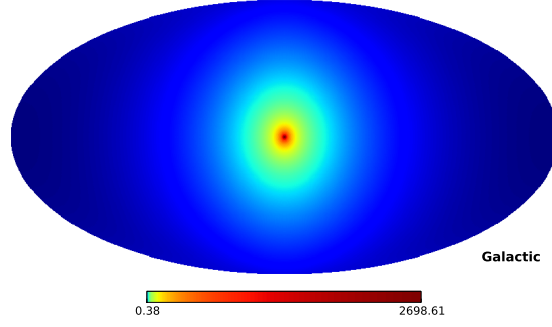


**Figure 1:** Dimensionless J-factor for annihilating DM as distributed in the Galaxy. The DM distribution is assumed to follow an Einasto profile. The Mollweide projection of the map is given in Galactic coordinates, centered on the position of the Galactic Center.

Here, we consider a simplified DM distribution, represented by a smooth Galactic DM halo. Other possible DM contributions such as DM accumulated in extragalactic halos are assumed to be subdominant. Point-source-like features such as possible Galactic DM subhalos (e.g., [14]) will be covered by our generic parameterization of  $dN/dS$ .

The Galactic DM density distribution  $\rho(r)$  was parameterized with an Einasto profile [15]. The dimensionless J-factor is given by

$$\mathcal{J} = \frac{1}{r_\odot} \int_{\text{los}} \left( \frac{\rho[r(l)]}{\rho_\odot} \right)^2 dl, \quad (2.2)$$

where  $r$  denotes the galactocentric radius and  $l$  is the line-of-sight, as measured from the Galactic position of the Sun. The J-factor is normalized to  $r_\odot$ , i.e. the galactocentric radius of the Sun, and  $\rho_\odot = \rho(r_\odot)$ . The J-factor obtained from Eq. 2.2 is shown in Fig. 1 as a function of the Galactic position. The observed gamma-ray flux from DM annihilation in the Galactic halo is then given by

$$\frac{d\phi_f}{dE d\Omega} = \frac{1}{4\pi} \frac{\langle \sigma v \rangle}{2} r_\odot \frac{\rho_\odot^2}{m_{\text{dm}}^2} \frac{dN_f}{dE} \mathcal{J}, \quad (2.3)$$

where  $\langle \sigma v \rangle$  denotes the thermally-averaged self-annihilation cross section for dark matter particles of mass  $m_{\text{dm}}$ . The differential gamma-ray spectrum  $dN_f/dE$  per unit energy interval  $(E, E + dE)$  yielded by pure annihilation into standard model final state  $f$  was taken from Ref. [16]. We considered annihilation into  $b\bar{b}$  quarks and  $\tau^+\tau^-$  leptons. The quantity  $x_{\text{dm}}^{(p)}$  can be derived from Eq. 2.3 and the exposure of the instrument.

### 3. Fermi-LAT Data

The counts map and the exposure map were produced from analyzing the first 8 years of gamma-ray data acquired with the Fermi-LAT. In particular, we used `PASS 8` data<sup>1</sup> and corresponding instrument response functions. Data reduction was conducted with the Fermi Science

<sup>1</sup><https://heasarc.gsfc.nasa.gov/FTP/fermi/data/lat/weekly/photon/>

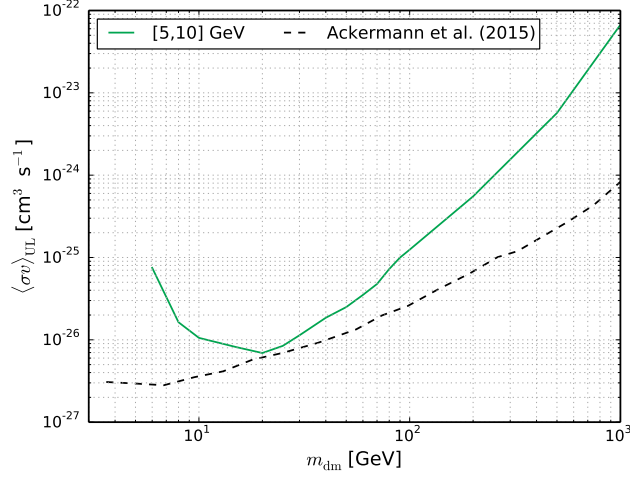


**Figure 2:** Sensitivity reach of the 1pPDF method for detecting an additional component of annihilating DM in the Galaxy. The solid green line depicts upper limits (95% CL) on the cross section  $\langle\sigma v\rangle$  of WIMPs annihilating to  $\tau^+\tau^-$  leptons. The upper limits have been obtained from the analysis of the 5-10 GeV energy band, employing the official IEM. The dashed black line depicts upper limits obtained from dwarf spheroidal galaxies, see Ref. [20].

Tools (v10r0p5)<sup>2</sup>. The analysis was restricted to events passing standard quality selection cuts, belonging to the ULTRACLEANVETO event class, and the PSF3 quartile. The contamination from the Earth’s limb was significantly reduced by requiring a maximum zenith angle of  $90^\circ$ . Events were binned in three adjacent energy intervals: (i) 1.04-1.99 GeV, (ii) 1.99-5.0 GeV, and (iii) 5.0-10.4 GeV. The counts map was pixelized using the equal-area HEALPix scheme [17], with a resolution parameter  $\kappa = 7$ .

In order to reduce systematic uncertainties, the region of interest (ROI) was restricted to Galactic latitudes  $|b| > 30^\circ$ . In addition, template models of the regions covered by the Fermi Bubbles [18] and Galactic Loop I [19] turned out to be equipped with high systematic uncertainties. We therefore excluded those regions from the ROI as well.

#### 4. Results

As a preliminary result of this analysis, Fig. 2 shows the sensitivity reach of the 1pPDF analysis for the 5–10 GeV energy bin and the example of the official IEM. The green curve shows upper limits on  $\langle\sigma v\rangle$  at 95% confidence level (CL), which were derived from fitting the previously explained representation of the gamma-ray sky with the 1pPDF method. No evidence was found for the additional DM component to significantly improve the quality of the fit, corresponding to an open, single-sided profile likelihood for the  $A_{\text{dm}}$  parameter. The corresponding upper limits on  $A_{\text{dm}}$  can be directly mapped into upper limits on  $\langle\sigma v\rangle$ , cf. Eqs. 2.1 and 2.3. Upper limits are shown for a DM particle mass range between 5 GeV and 1 TeV.

<sup>2</sup><https://fermi.gsfc.nasa.gov/ssc/data/analysis/software/>

Fig. 2 can be interpreted as the sensitivity reach of the 1pPDF method between 5 and 10 GeV, under the assumption that systematic uncertainties of the official IEM used here to model the Galactic foreground emission are comparably small and do not absorb any additional DM component. The analysis will significantly improve when considering lower energy bands, providing significantly higher event statistics. In particular, a joint analysis of all energy bands is expected to further reduce possible correlations between the IEM and the additional DM component, given the different energy spectra of the two components.

We find that the sensitivity reach of the 1pPDF method is competitive to limits recently obtained from dwarf spheroidal galaxies [20], see black dashed line in Fig. 2.

## Acknowledgments

HSZ gratefully acknowledges the Istituto Nazionale di Fisica Nucleare (INFN) for a post-doctoral fellowship in theoretical physics on "Astroparticle, Dark Matter and Neutrino Physics", awarded under the INFN Fellowship Programme 2015.

## References

- [1] Fornasa, M., & Sánchez-Conde, M. A. 2015, *Phys. Rep.*, 598, 1
- [2] Ackermann, M., Ajello, M., Albert, A., et al. 2015, *ApJ*, 799, 86
- [3] Acero, F., Ackermann, M., Ajello, M., et al. 2015, *ApJS*, 218, 23
- [4] Ajello, M., Shaw, M. S., Romani, R. W., et al. 2012, *ApJ*, 751, 108
- [5] Ajello, M., Romani, R. W., Gasparrini, D., et al. 2014, *ApJ*, 780, 73
- [6] Ajello, M., Gasparrini, D., Sánchez-Conde, M., et al. 2015, *ApJ*, 800, L27
- [7] Malyshev, D., & Hogg, D. W. 2011, *ApJ*, 738, 181
- [8] Selig, M., Vacca, V., Oppermann, N., & Enßlin, T. A. 2015, *A&A*, 581, A126
- [9] Lee, S. K., Lisanti, M., Safdi, B. R., Slatyer, T. R., & Xue, W. 2016, *Physical Review Letters*, 116, 051103
- [10] Lisanti, M., Mishra-Sharma, S., Necib, L., & Safdi, B. R. 2016, *ApJ*, 832, 117
- [11] Zechlin, H.-S., Cuoco, A., Donato, F., Fornengo, N., & Vittino, A. 2016, *ApJS*, 225, 18
- [12] Zechlin, H.-S., Cuoco, A., Donato, F., Fornengo, N., & Regis, M. 2016, *ApJ*, 826, L31
- [13] Bertone, G., Hooper, D., & Silk, J. 2005, *Phys. Rep.*, 405, 279
- [14] Zechlin, H.-S., Fernandes, M. V., Elsässer, D., & Horns, D. 2012, *A&A*, 538, A93
- [15] Einasto, J. 1965, *Trudy Astrofizicheskogo Instituta Alma-Ata*, 5, 87
- [16] Cirelli, M., Corcella, G., Hektor, A., et al. 2011, *J. Cosmology Astropart. Phys.*, 3, 051
- [17] Górski, K. M., Hivon, E., Banday, A. J., et al. 2005, *ApJ*, 622, 759
- [18] Su, M., Slatyer, T. R., & Finkbeiner, D. P. 2010, *ApJ*, 724, 1044
- [19] Casandjian, J.-M., Grenier, I., & for the Fermi Large Area Telescope Collaboration 2009, arXiv:0912.3478
- [20] Ackermann, M., Albert, A., Anderson, B., et al. 2015, *Physical Review Letters*, 115, 231301